Model-based auralizations of violin sound trends originating from plate tuning and from bridge tuning

Robert Mores, University of Applied Sciences, Hamburg, Germany

Robert.Mores@haw-hamburg.de

Abstract

Luthiers routinely tune ring- and X-modes of top and back plates (pre-assembly) as well as the bridge (post-assembly, with sound post), and usually they consider these two as being the most important determiners of sound. Plate modes relate to plate thickness and therefore to the critical frequency f_{crit} for radiation. Empirical data on relations between air modes, non-assembled plate modes, and body modes encouraged parametric modelling of a violin radiativity profile $R_{DF}(f)$ using only the two parameters f_{crit} and f_{rock} (bridge) to capture general sound trends [Bissinger, JASA, 2012]. $R_{DF}(f)$ is transformed to a minimal-phase non-ringing FIR filter to auralize related sound trends while varying these two parameters. Auralizations were created by applying this filter to a bowed-string driving force measured at the bridge of a solid-body violin.

Introduction into the underlying model

How does thinning the violin's top and back plate thicknesses affect its sound? Surprisingly there is no simple answer to this question, given the additional effects of plate arching, sound post placement, bridge tuning, etc, in the ultimate bowed instrument sound.

Nor has there been much help from the theoretical side. Profound difficulties remain in creating any analytic model of violin radiation: non-analytic shapes of the various substructures, nominally orthotropic wood materials with variable density and grain angle, reliable extraction of the nine independent elastic moduli, characterization of joints, stress loading of bridge and sound post, the bridge-corpus interaction, a physical mechanism for cavity mode excitation.

Given these difficulties we chose a workable alternative: treat only the general aspects of measured violin vibration and radiation properties in a basic structural acoustics context, defining the violin in effect not by what it is – materials, shape, construction – but *by what it does* – using a comprehensive range of excited-at-bridge dynamics, vibration and radiation, all integrated into a "dynamic filter" (DF) model[1] for violin radiativity. Implicit in this model of violin radiativity is the underlying notion that applying a driving force at the bridge, as in bowing, will return a perceivable pressure, a sound.

The necessity to place any model of violin sound into a structural acoustics[2] context can be argued from one key example, viz., the effect of "tuning" the top and back plates of the violin prior to assembly. Plates graduated towards the thick end of the usual range will move the assembled corpus (top + ribs + back) modes toward higher frequencies, simultaneously lowering the plate critical frequency f_{crit} – where the bending wave catches up with speed of sound and vibrational energy transformation into radiation maximizes – due to the dispersive bending waves increasing in velocity as $\sqrt{f}$ (all frequencies f in Hertz). Tuning plates toward the thin side has the converse effect.

Experimental examples of such "low-high" behavior appeared in 1991 when Dünnwald presented 10-violin superposition plots[3] of excited-at-bridge, single-microphone pressure measurements for *i)* old-Italian violins (a nominal standard of quality), characterized by consistent low-lying corpus mode radiative behavior and a high frequency output that fell between *ii)* master maker violins, whose corpus mode frequencies tended to fall below old-Italian values but with a much-extended high frequency output, and *iii)* factory violins, typically with over-thick plates, whose corpus mode frequencies fell higher than old-Italian corpus mode frequencies but with a much-contracted high frequency output. The excellent agreement between DF model simulations for plate tuning (shown later) and general trends observed in these 10-violin subsets – e.g., the factory violins showed relatively weak A0 and weak response above 3 kHz – provides strong validation of the model and its inclusion of structural acoustics.

The DF model was developed to account for radiative behaviors observed for experimental mean-square, averaged-over-sphere total (*f*-holes + surface) radiativity profiles $\langle R(f)^2 \rangle$ for 17 violins (r = 1.2 m, anechoic chamber, "unconstrained" *free-free* suspension), paired with simultaneous EMA mean-square, 14-violin average-over-corpus violin mobilities $\langle Y(f)^2 \rangle$ (Y(f) is the frequency-dependent complex ratio of surface normal velocity to driving force).

Having $\langle R(f)^2 \rangle$, $\langle Y(f)^2 \rangle$ and their *ratio* significantly expanded the applicable structural acoustics to include radiation efficiency, critical frequency and statistical energy analysis (SEA) concepts[2]. Some of the most important general results incorporated in the DF model include:

1) below ~600 Hz - the open string *deterministic* region with five well-separated "signature" modes readily tracked from violin to violin; three of which always radiated strongly, viz., the violin's compliant wall Helmholtz resonator A0, near 275 Hz and two large volume-change, 1st corpus bending modes $B1^-$ and $B1^+$, nominally near 470 and 540 Hz, resp. A0, $B1^-$ and $B1^+$ radiate completely (A0) or primarily (the B1 modes) through the *f*-holes[4]. In addition, A1, the 1st longitudinal cavity mode near 470 Hz radiates through induced wall motions but rarely strongly[4]; it is important because it couples to A0. The CBR mode near 400 Hz doesn't radiate significantly and is neglected. In the DF

model cavity volume flows induced by B1 wall motions only, which also contribute B1 surface radiation, are employed in a wall-driven, dual-Helmholtz resonator network model for A0 *f*-hole radiation[1]. The complexity of the signature mode region can be seen directly in the experimental mode veering diagrams[5] of Weinreich, Holmes and Mellody that exposed significant interactions between A0 and the B1 modes; 2) from ~600 to ~ 800 Hz - a featureless radiativity 'trough" where $<R(f)> \approx 0.19$ Pa/N at 630 Hz for all violin quality classes in the 17-violin dataset [1]; and 3) above ~800 Hz - a *statistical* region with: *i)* much modal overlap, *ii)* unreliable mode tracking across violins, *iii)* the major effects of bridge rocking frequency (f_{rock}) tuning, *iv)* band-average modal properties parameterized via trend lines, and *v*) applicable SEA methods-formulas.

In the deterministic region the computed DF model radiativity "profile" $R_{DF}(f)$ reliably predicts A0 strength[1] . The statistical region DF model starts with the mathematical identity, viz., $<R(f)^2> = <Y(f)^2> \bullet \{<R(f)^2>/<Y(f)^2>\}$, with subsequent relevant structural acoustics parameter substitutions while still retaining its identity character. The RHS 1st term provides a gauge of mode/band excitation, while the 2nd {} term leads to the radiation efficiency $R_{eff}(f)$, the violin's effective critical frequency f_{crit} and the radiation damping $\zeta_{rad}(f)$. The bridge filter effect[6] inherent in bridge-excitation vibration-radiation measurements was emphasized by introducing a *distributed-excitation* statistical mobility function[2] Y_{stat}^2, giving $<R(f)^2> = <Y(f)^2>\bullet\{<R(f)^2>/<Y(f)^2>\}\bullet Y_{stat}^2/Y_{stat}^2 = (<Y(f)^2>/Y_{stat}^2) \bullet\{<R(f)^2>/<Y(f)^2>\}\bullet Y_{stat}^2$. The RHS ( ) term becomes the "shape" function, $\Phi(f) = <Y(f)^2>/Y_{stat}^2$. A "scaling" function S(f) accommodates bridge rocking frequency changes from the nominal initial f_{rock} [1].

Y_{stat}^2 introduces easily modifiable "global" parameters: a) modal density *n*(f), the number of modes per 250 Hz band, b) violin total mass M ≈ 0.4 kg, which varies with plate tuning, and c) total damping $\zeta_{tot}(f) \propto f^{-0.34}$ from fits to experimental mobility data. $\zeta_{tot}(f)$ sums over $\zeta_{rad}(f)$, internal (heat) damping $\zeta_{int}(f)$, (and support fixture damping $\zeta_{fix}(f)$, not considered here). To quantify the fraction-of-vibrational-energy-radiated the parameter $F_{RAD}(f) = \zeta_{rad}(f)/\zeta_{tot}(f)$ was introduced. Near the violin's effective critical frequency $\zeta_{rad}(f)$ and $F_{RAD}(f)$ both pass through a maximum, and the violin most efficiently turns vibrational energy into radiation. The statistical region radiativity profile was computed from $R_{DF}(f) \propto [\Phi(f) \bullet n(f) \bullet S(f) \bullet F_{RAD}(f)/M]^{1/2}$. $R_{DF}(f)$ now "filters" raw string vibrations and naturally includes any "bridge filter" effects in $<R(f)^2>$ and $<Y(f)^2>$.

Auralizations for various violin parameter changes in the DF model now require only convolving each computed $R_{DF}(f)$ with the measured bowed-string driving force $F_{bow}(f)$. These auralizations still retain much essential violin sound character due to the attack-decay-sustain-release transients and phase information in the "stick-slip" driving force, even though model simplifications clearly must reduce complexity in the simulated violin sounds. A major point here is that the realistic bowed-string driving force common to all auralizations serves to emphasize perceived qualitative *trends* in violin sound that accompany stepped changes in $R_{DF}(f)$ due to *only* plate tuning, or *only* bridge tuning.

Auralization

To convert R_{DF} calculations into auralizations the procedural steps outlined in the appendix arrive at linear-phase, low-delay, non-ringing FIR filters that can be directly convolved with driving force signals from bowed strings. Stepped-parameter auralizations then expose the sound trends.

These auralizations require a bowed string driving force $F_{bow}(f)$ consistent with the radiativity measurements. Placing a transducer at each string termination introduces significant crosstalk, while at the same time each transducer needs its own specific equalization function to compensate for the "acoustic fingerprint" of the violin used to record samples since the DF-modeled violin is to be auralized , not the violin used for playing. A single transducer at the waist of a conventional bridge (inset Figure 1): *i)* avoids cross-talk, *ii)* is favorably close to the strings, and *iii)* can be instrumented for the equalization task. The instrumented bridge was mounted on a Yamaha model SV 200 solid body violin (mass = 0.65 kg vs. the ~0.07 kg spruce top of the traditional violin) of low structural complexity to minimize any "acoustic fingerprint" from feedback to the waist transducer. The transducer signal supplies the bowed string driving force (sound samples of this signal on author's home page: first eight bars of J. S. Bach's Double from Partita No. 1, BWV 1002).

Although violin bridge "filter" effects rival the effects of plate tuning[1] (as will be seen) only the bridge top filter function $\Gamma_{top}(f)$ is important here, as expressed in $F_{waist}(f) = F_{bow}(f) \times \Gamma_{top}(f)$. $\Gamma_{top}(f)$ was estimated from frequency response functions measured for mini-force hammer impacts at the E and G string bridge sides and the in-waist transducer response. The original bowing force was retrieved by applying the serial inverse filter $\Gamma_{top}(f)^{-1}$ to $F_{waist}(f)$, i.e., $F_{bow}(f) = F_{waist}(f) \times \Gamma_{top}(f)^{-1}$.

Auralizations of DF model simulations were created for three important stages of violin development: Stage 1) *pre*-assembly thick-intermediate-thin plate tuning (anechoic chamber R_{DF}), and Stage 2) *post*-assembly f_{rock} tuning 2.6-3.0-3.4 kHz (anechoic chamber R_{DF}). All simulations assume a properly set up traditional violin.

Stage 1: pre-assembly - plate tuning

The physical effects of plate graduation are straightforward. Thicker plates (with higher mass) lead to higher assembled-violin mode frequencies, somewhat reduced mechanical response and weakened A0 excitation. Thicker plates also lead to lower critical frequencies, reducing high frequency response above the critical frequency f_{crit}. The R_{DF} simulations for plate tuning effects range from: a) thick plate violins with plate mode #5 ≈ 400 Hz consistent with a machine-figured (factory) student violin and $f_{crit} \approx 2$ kHz, to b) intermediate plate violins with mode #5 ≈ 360 Hz and $f_{crit} \approx 3.3$ kHz, to c) thin plate violins with mode #5 ≈ 340 Hz and $f_{crit} \approx 4.6$ kHz. Note that relatively large f_{crit} changes

accompany relatively small mode #5 frequency changes. Figure 1 presents the three plate tuning radiativity profiles (sound samples are provided[9]).

The R_{DF} curves in Figure 1 (f_{rock} = 3.2 kHz) reliably represent experimental trends for the 17-violin-average radiativity profile over the various violin quality classes. Changes near 1 kHz come from an ~13% mass decrease accompanying thick → thin plate tuning.

Overall, thick plates substantially decrease R_{DF} above f_{crit} = 2 kHz as radiation damping above f_{crit} falls off as 1/f. Somewhat smaller decreases occur in the A0-B1 region, signalling relatively weaker low and high frequency regions, consistent with the Dünnwald 10-factory violin dataset. (Perceived sound evolution for f_{crit} = 4.6 kHz → 2.0 kHz is especially revealing.)

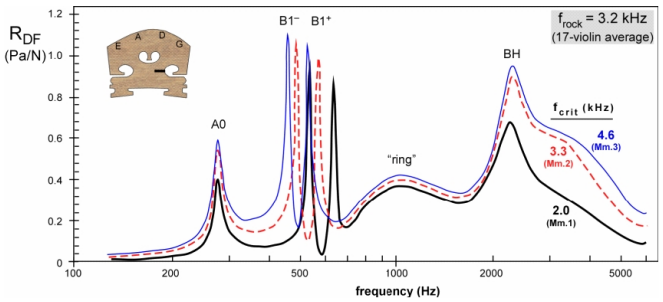

Figure 1: Effect of plate tuning on the violin's anechoic chamber radiativity profile (f_{rock} = 3.2 kHz.): "thick" (thick line) with f_{crit} = 2 kHz, "intermediate" (thin dashed line) with f_{crit} = 3.3 kHz and "thin" (thin line) with f_{crit} = 4.6 kHz. (A bowed-string excitation sound (wav) file accompanies each profile.) Labels: deterministic region - signature modes A0, $B1^-$ and $B1^+$; statistical region major structures - fixed frequency "ring" and BH, and variable frequency f_{rock}. (Inset: transducer position blackened in bridge waist.)

Stage 2: post-assembly - bridge tuning

The stepped-f_{rock} simulations in the model use systematic experimental measurements[6] since no reliable theoretical model exists. Stepping the rocking frequency f_{rock} from 2.6 → 3.0 → 3.4 kHz as in Figure 2 produces R_{DF} trends quite similar to those seen in Figure 1 for plate tuning. Higher f_{rock} (thicker waist) increases the radiativity considerably more at high frequencies than low. All bridge tuning simulations used f_{crit} = 3.9 kHz, the bad-good-excellent 14-violin average result[1]. Two important insights into violin sound now emerge, viz., tuning low frequency modes of the top and back plates simultaneously affects both the low *and* high ranges of violin response; similarly, tuning the high frequency f_{rock} affects both the high *and* low ranges. Thus some plate tuning outcomes can be compensated for to some extent by compensatory bridge tuning, a possible rationale for why plate tuning remains a somewhat murky area. Figure 2 presents the three bridge tuning radiativity profiles (sound samples are provided[9]).

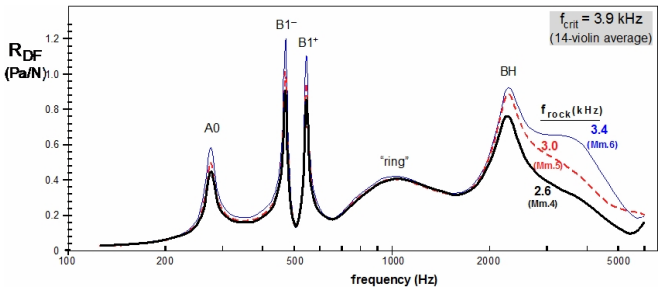

Figure 2 : as in Figure 1, but f_{crit} fixed at 3.9 kHz and f_{rock} varied from 2.6 kHz (thick line) to 3.0 kHz (thin dashed line) to 3.4 kHz (thin line).

Summary

In summary these first model-based auralizations of violin sound use a realistic bowed-string driving force and provide a perceptual acoustic sense of the purely mechanical plate or bridge tunings that complement the dynamic filter model's visualized radiativity profiles. Deterministic and statistical regions of violin spectra are modelled from empirical data to reveal trends rather than details.

References and links

1 G. Bissinger, "Parametric plate-bridge dynamic filter model of violin radiativity", J. Acoust. Soc. Am. **132**, 465-476 (2012).

2 F. Fahy and P. Gardonio, *Sound and Structural Vibration: Radiation, Transmission and Response*, 2nd ed. (Academic Press, 2007, New York).

3 H. Dünnwald, "Deduction of objective quality parameters on old and new violins", Catgut Acoust. Soc. J., Vol. **1**, No. 7(Series II): 1-5 (1991).

4 G. Bissinger, E.G. Williams and N. Valdivia, "Violin *f*-hole contribution to far-field radiation via patch near-field acoustical holography", J. Acoust. Soc. Am. **121**, 3899–3906(2007).

5 G. Weinreich, C. Holmes, and M. Mellody, "Air-wood coupling and the swiss-cheese violin", J. Acoust. Soc. Am. **108**, 2389-2402(2000).

6 G. Bissinger, "The violin bridge as filter", J. Acoust. Soc. Am. **120**, 482-491 (2006).

7 K. D. Marshall, "The musician and the vibrational behavior of the violin", Catgut Acoust. Soc. J., **45**, 28-33(1986).

8 A.V. Oppenheim, R.W. Schafer, *Programs for Digital Signal Processing*, IEEE Press, John Wiley & Sons, 1979, algorithm 7.2.

9 URL *http://www.mt.haw-hamburg.de/akustik /download/DAGA_2015_violin_auralization/*

Appendix - Converting $R_{DF}(f)$ into minimum phase filters

The process to convert $R_{DF}(f)$ calculations into minimum-phase filters follows this five-step procedure:

- Zero-pad $R_{DF}(f)$ down to DC if necessary (our data holds information only for frequencies between 125 Hz and 6,000 Hz, at a resolution of 1 Hz). The real part of the coefficient set in the frequency domain is $A_k = 0$ for $k = 0, \ldots, 124$, and $A_k = R_{DF}(f)$ for $k = 125, \ldots, 6{,}000$. This coefficient set of length $N = 6{,}000$ is mirrored to also represent corresponding negative frequencies while obeying the periodical-spectrum paradigm of discrete transforms. $A_{2N-k} = A_k$ for $k = 1, \ldots, N - 1$. The imaginary part $B_k = 0$ for $k = 0, \ldots, 11{,}999$. The data set now holds $2N = 12{,}000$ complex coefficients.
- Apply an inverse discrete Fourier transformation (IDFT) resulting in a coefficient set $a[n]$, $n = 0, \ldots, 2N - 1$ with only real parts and no imaginary parts. This set represents a time signal of 1 s duration at 12 ksamples/s. As a result the desired violin impulse response will be found in two halves, at the two sides of $a[n]$.
- Proper concatenation of the two halves results in a symmetric impulse, $a[n] = a[2N+n]$ for $n = -N, \ldots, -1$, centered around $n = 0$, and represented in the range $n = -N, \ldots N - 1$. To achieve causality, the set should finally be shifted, $a\_causal[n] = a[n-N]$ for $n = 0, \ldots, 2N - 1$. This impulse response has a linear phase and zero group delay but some delay with the potential of ringing, since some hundred coefficients ahead of the main impulse already have significant values. Such an ascending signal would be annoying.
- Flipping this pre-impulse fraction of the impulse response and adding to the post-impulse side achieves an initial impulse followed by a declining envelope and some subsequent instrumental reverberation. Such flipping however creates a too instantaneous impulse at $t = 0$ causing an annoying clicking. Therefore, the left (right) side of the impulse is ramped down (up) with a psycho-acoustically neutral 10 ms ramp in form of a $\pi/2$ cosine, prior to flipping. The ramp is applied to the coefficient set prior to shifting, when the impulse is still symmetric around $n = 0$. For a ramp of length $2M + 1$ we use $r[n] = 0.5 + 0.5 \cdot \sin(\pi \cdot n/2M)$ for $n = -M, \ldots, M$, extended by zeroes to the left side, $r[n] = 0$ for $n = -N, \ldots, -M$, and extended by ones to the right side, $r[n] = 1$ for $n = M, \ldots, N - 1$. The impulse response is now weighted with the ramp, $a\_r[n] = a[n] \cdot r[n]$, but also with the flipped ramp, $a\_rf[n] = a[n] \cdot r[-n]$. Flipping and adding $a\_rf[n]$ to $a\_r[n]$ is equivalent to doubling $a\_r[n]$, since $a[n]$ was symmetric around $n = 0$. Note, that $r[n] + r[-n] = 1$ for all n. The impulse is now non-ringing *and* psycho-acoustically prepared. The coefficient set $2 \cdot a\_r[n]$ has a linear phase and a much smaller delay. The shifting for causality now only takes the ramp into account, $a\_causal[n] = 2 \cdot a\_r[n-M]$ for $n = 0, \ldots, N + M - 1$.
- This impulse response now serves as the DF filter to be convoluted with the bowed string driving force obtained from a solid body violin in the time domain. The sound was re-sampled to match the 12 ksamples/s as defined by the data size of $R_{DF}(f)$.

As an alternative to the outlined method the Kolmogerov method[8] also achieves minimum-phase, single-sided, low-delay impulse responses. The Kolmogerov method is widely used and commonly known as real cepstrum (MATLAB function *rceps*) requiring the first three preparation steps as described and requiring a post-processing to effectively prevent the echo that comes along when using *rceps*. However, with this method, the phase is not linear anymore, and the impulse responses reveals a dark sound (A0 and signature modes are overemphasized). The reason for this is that the minimal phase only holds for frequencies below the first resonances, while higher frequencies are delayed, see figure 3 the phase in the right column. Even though the results from the two methods are numerically the same in terms of their spectral magnitude, the auditory event differs due to the different phase. Perceptually the flipped IR is very close to the symmetrical IR obtained from IDFT, while the minimum-phase IR is not. Therefore, the flipping method is preferred for the appended sound samples.

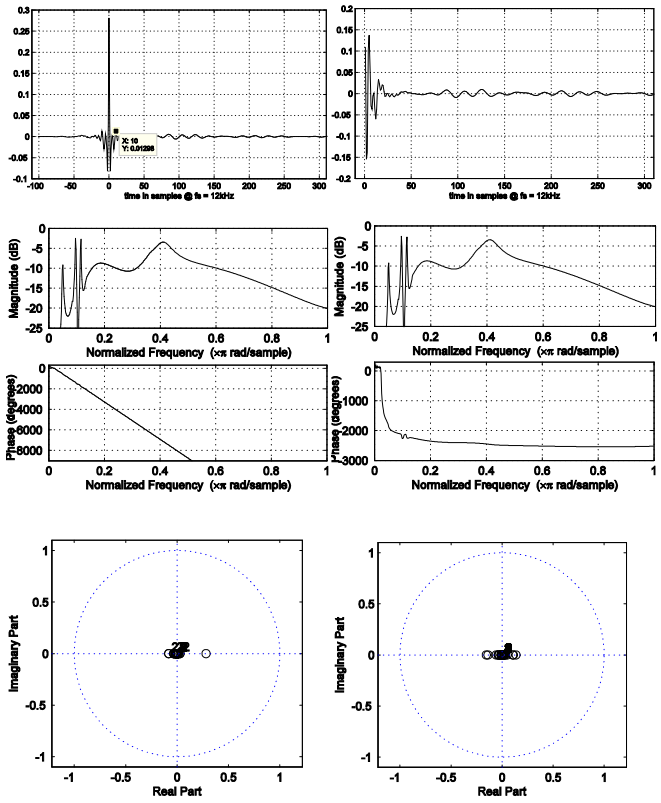

Figure 3 : comparison of the two methods, "flipping" method (left column) and "real cepstrum"(right column), from the top: impulse response in the time domain, in the frequency domain magnitude and phase, and the associated roots represented in the complex plane.